Energy Loss of Low Energy Protons on LiF(100): Surface Excitation and H^- Mediated Electron Emission

P. Roncin,* J. Villette, J. P. Atanas, and H. Khemliche

Laboratoire des Collisions Atomiques et Moléculaires (CNRS UMR 8625), Batiment 351, Université Paris Sud, F-91405, Orsay Cedex, France

(Received 8 January 1999)

Impact of 600 eV protons at grazing incidence on LiF(100) is studied with a new coincidence technique combining energy loss and electron spectroscopy. Correlation between the secondary electrons and the charge state of the scattered projectiles demonstrates the role of the H^- ions formed on the surface as precursors for electron emission. However, the main channel for energy loss is not associated with electron emission but is interpreted as the population of surface excitons.

PACS numbers: 79.20.Rf, 34.50.Dy, 34.70.+e, 73.20.–r

Since the pioneering work of Souda *et al.* [1] ten years ago, the study of low-energy ions interacting with large band gap insulators and the subsequent energy loss and electronic emission has attracted much interest [2–7]. Compared to metallic surfaces, the large band gap and high binding energies of the valence electrons are expected to induce profound differences from several aspects: (i) The energy loss (through electronic stopping) of ions traveling along the surface should exhibit a threshold behavior with incident energy. (ii) The ion velocity threshold for kinetic electron emission is expected to increase with respect to that of metals. (iii) The resonant electron transfer (from and to the solid) should be strongly reduced. Points (i) and (ii) are simply due to the much larger energy required to excite or ionize valence electrons. The most recent observations by Auth *et al.* [8] have confirmed point (i) in collisions of protons with LiF but with a threshold behavior appearing only at substantially lower energy than expected [9]. With respect to point (ii), Vana *et al.* [2] showed that no clear energy threshold can be observed in the secondary electron emission yield during singly charged ions (H^+, Ar^+) collision on LiF, whereas a threshold of 1 keV was measured for the same projectiles on Au. As for charge exchange, the resonant neutralization of singly charged alkali ions and the resonant ionization of alkali atoms is strongly reduced because of the band gap [10]. The suppression of this electron loss channel is also partly responsible for the surprisingly large negative ion fractions, up to 60%–90% [11,12] observed for oxygen or fluorine interacting with alkali halides. The capture process was elucidated only recently as being due to a lowering of the projectile affinity level in the Madelung potential [8,13,14].

The presence of a large band gap indeed controls the resonant electron capture and loss but does not seem to play the same decisive role in the energy loss or in the electron emission. This paradox has been studied in detail for the H^+-LiF system, which may be considered as a reference. The projectile has a well-known electronic structure, and since the LiF band gap extends above the vacuum level, energy loss and electron emission should be intimately related. These studies have called for the existence of an intermediate state able to reduce the effective band gap during the collision process. On one hand, independent measurements of secondary electron yields [15] and stopping power at energies above 2 keV [9] have both been explained using an excitation scheme without electron capture. On the other hand, from energy loss measurements below 1 keV, Auth *et al.* [8] have proposed a scheme with successive cycles of capture to and loss from H^-, thus assuming the negative ion to be the precursor for both electron emission and energy loss.

Combining coincidence energy loss and electron spectroscopy, we present in this Letter experimental evidence for negative ion-mediated electron emission for grazing collisions of protons on LiF. We also demonstrate that most of the electrons removed from the valence band remain on the surface, in states identified as surface excitons, leading to energy loss without electron emission.

The main part of the experimental setup [16] is composed of 16 microchannel plate detectors mounted on a hemisphere surrounding the target and placed in a UHV μ-metal chamber. The 600 eV proton beam is chopped, reduced to a size of 100 μm, and sent to the LiF(100) target at incidence angles between 0.4° and 2.9°, thus keeping the normal energy below 3 eV. The scattered beam passes a slit perpendicular to the surface plane where it is charge-state analyzed by a set of plates parallel to the slit. The coordinates of the projectile's impact onto a two-dimensional position-sensitive microchannel plate detector (PSD) provide the scattering angle and the charge state. For calibration purposes, the collision geometry is such that a small fraction of the incident beam strikes the PSD without interacting with the surface. Electrons emitted from the target drift freely to the 16 hemisphere detectors where they are accelerated to 400 eV just before striking the microchannel plates. All the detectors' outputs as well as the chopper signal are recorded in a 32 channel multihit time-to-digital converter. The energies of all detected particles are determined

 0031-9007/99/83(4)/864(4)$15.00

independently by their time-of-flight referred only to the chopper signal.

The scattering profile is sharply peaked around the specular direction, its width being used to check the quality of the surface following cycles of grazing sputtering by 5 keV Ar^+ ions and annealing at 400 °C. During the experiment, the target temperature is kept above 250 °C to allow for sufficient ionic conductivity. The unscattered direct beam is taken as a reference for the energy loss. However, since different charge states follow different paths to the PSD, a possible error, estimated here to be below 3 eV, may arise when comparing different final charge states. We also check on-line that the detection efficiency of the PSD is not too sensitive to the projectile charge state. To calibrate the electron detection efficiency, we used immediately after the experiment an *in situ* alpha source for generating secondary electrons through a thin aluminum foil [17]. From this detection efficiency, a regular matrix transforms the energy loss spectra recorded in coincidence with 0, 1, or 2 electrons *detected* into energy loss spectra correlated with 0, 1, or 2 electrons *emitted*.

Such corrected energy loss spectra of H^0 and H^- particles are displayed in Fig. 1 for 600 eV protons impinging at 2.9° incidence on LiF(100) oriented along a high index direction. The fractions of scattered H^0, H^-, and H^+ particles amount to 97.5%, 2.5% ± 0.7%, and below 0.2%, respectively. For simplicity, we note (H^q, n) the energy loss spectrum of H^q associated with *n emitted* electrons.

As the most salient feature, we observe for all spectra well-resolved structures regularly spaced by 11.9 ± 0.2 eV, whereby $(H^0, n + 1)$ is shifted by ≃3 eV with respect to (H^0, n). The first peak around 1.5 eV in $(H^0, 0)$ is related to the quasiresonant neutralization of the incident H^+. As already noted for more grazing angles where this peak is dominant [8], its position does not exactly match the pure electronic energy defect and therefore implies nonelectronic interactions [18], which are beyond the scope of the present Letter. All the other peaks correspond to quantized energy losses induced by the removal of valence electrons and confirm the strong indications found in [8]. The interpretation in terms of successive cycles of electron removal from the valence band becomes clear when noting the absence in $(H^q, n + 1)$ of the lowest energy peak of (H^q, n). This simply recalls that valence electrons have to be extracted before they can be emitted. Similarly, (H^-, n) misses the lowest energy peak of (H^0, n), indicating that the attached electron also originates from the valence band. Each peak can then be assigned to a well-defined number of electrons removed from the valence band. The mean number of extracted electrons is 1.5, and the probability distribution for the removal of n electrons is well reproduced by the binomial law $\binom{n}{n_s}\mathbf{P}^n(1 - \mathbf{P})^{n_s - n}$, provided the statistical ensemble n_s is on the order of 10 and $\mathbf{P}$ is close to 15% (more precisely $1.5/n_s$). n_s is interpreted as the number of lattice sites visited and $\mathbf{P}$ as the mean probability *per lattice site* to extract a valence electron. The trajectory can be calculated with the scattering potential described in [8], then the value of $n_s = 10$ corresponds to active distances to the surface $2 \leq Z \leq 3.5$ a.u.

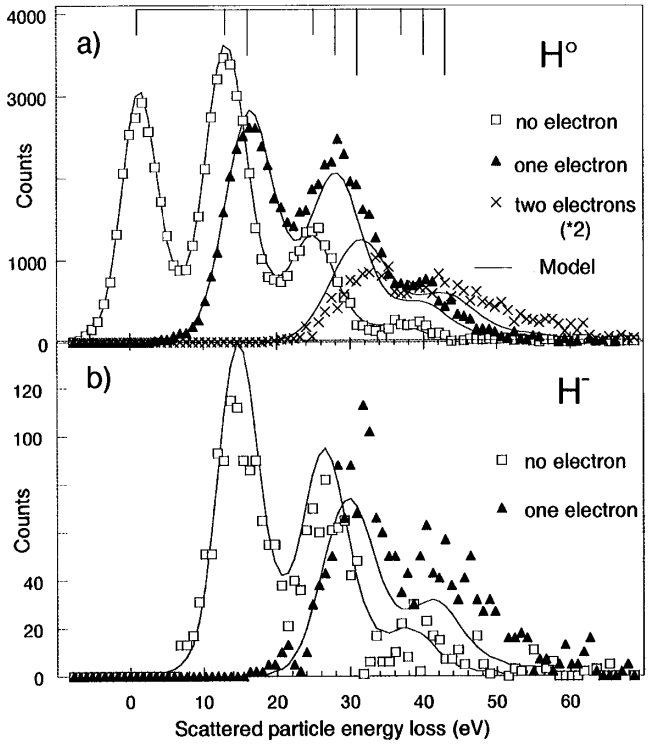

FIG. 1. Energy loss spectra of scattered H^0 (a) and H^- (b) associated with zero (□), one (▲), and two (×) electrons emitted; the full curve is from the H^- model (see text). (Note that both the experiment and the model associated with two emitted electrons have been multiplied by 2.) The vertical lines indicate the peak positions.

More surprising, the $(H^0, 0)$ spectrum shows that the projectile can lose a large amount of energy without emitting secondary electrons. In fact, most extracted electrons are not emitted, a mean value of 0.4 electron emitted per electron extracted is measured. For a given number n of electrons extracted, the probability to emit p electrons is well reproduced by $\binom{p}{n}\mathbf{B}^p(1 - \mathbf{B})^{n-p}$, with $\mathbf{B} = 0.4$. Following each electron removal from the valence band, $\mathbf{B}$ is the probability or branching ratio for this electron to end up in vacuum. The full curves in Fig. 1(a) correspond to the product of these two binomial laws, together with the peak position given by that of the quasielastic peak shifted by 12 or 15 eV depending on whether the electron is emitted or not.

The electron energy spectrum is a smooth distribution peaked around 1 eV and with a mean value close to 2 eV. Figure 2 displays a two-dimensional plot of electron energy versus energy loss of H^0 *referred to the quasielastic peak*. Superimposed is a linear fit to the data with a slope of 0.97 ± 0.10 eV/eV. This energy conservation

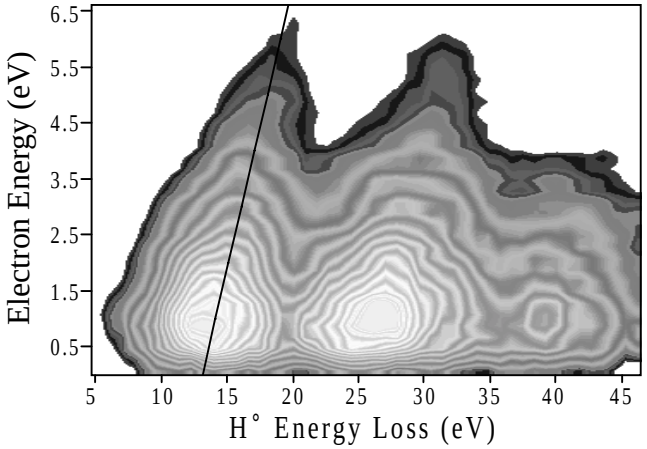

FIG. 2. Two-dimensional plot of the electron energy versus energy loss of scattered H^0. The unit slope of the linear regression (full line) indicates that the energy is shared between the ion and the electron.

means that the emitted electrons do not suffer inelastic collisions. For zero electron energy, the line extrapolates to a mean energy loss of 13 ± 0.3 eV. This is in good agreement with the location of the center of the surface valence band measured by metastable induced electron spectroscopy [19]. Comparing with the peak separation of 11.9 ± 0.2 eV when no electron is emitted, we derive a mean binding energy of 1.1 ± 0.5 eV for the states that trap the electrons at the surface.

This value is too large for image states owing to the small dielectric response function of LiF [7]. Moreover, the inhibition of electron loss from slow alkali atoms [10] seems to exclude the existence of empty surface states in this region. Surface excitons however explain the present findings; they correspond to excited states of the $F^0 + e^-$ system in the local positive Madelung potential rather than to empty surface states. Our binding energy of 1 eV is consistent with the threshold excitation energy around 10 eV (i.e., from the top of the valence band) measured by electron impact [20,21]. Though, to our knowledge, the population of excitons has never been observed in ion-surface scattering, this process is found here to be the *dominant* channel for energy loss.

The present findings do not explain how these states are populated. Since both the exciton population and the electron emission unambiguously require more than 10 eV, we approve the conclusion that an intermediate electronic state of the H^0-F^- system is probably responsible for bringing valence electrons up to (near) vacuum [8,9,15]. The promotion model [15] explains the electron emission via molecular autoionization of promoted $F^-(2p)$ electrons during H^0-F^- close collisions, whereas the H^- model [8] relies on successive cycles of electron capture onto H^- and subsequent detachment. After proper account of the branching ratio **B** for an electron extracted from the valence band to end up in vacuum or in the exciton states, these two models fit extremely well the (H^0, n) energy loss spectra. However, both models need refinement to reproduce the observed H^- fraction. Negative ions are not considered by the promotion model, but the addition of a small attachment probability on the order of $0.025/n_s$ per lattice site is enough to build up the observed H^- fraction. Alternatively, when fitted to the (H^0, n) spectra the H^- model [8] predicts a charge state equilibrium on the surface larger than that observed. This suggests that, on the outgoing part of the trajectory, the negative ion can still detach its electron at distances from the surface where capture is no longer active (here $Z > 3.5$ a.u.). Thus, the agreement is obtained by introducing a survival probability on the order of 18% for the H^- ions to leave the surface without losing their electron. Then both models fit equally well the (H^0, n) spectra and the charge fraction, but they do not predict the same number of emitted electrons associated with an H^- product. In the promotion model, H^0 is the only presumed precursor for electron emission, and the small H^- fraction on the surface is assumed to be stable. The H^- ions detected have been formed anywhere along the trajectory; thus, on average an H^- product has spent only half of the time on the surface as H^0. As a direct consequence, this model predicts a mean number of 0.2 electrons emitted per negative ion, less than half the 0.48 ± 0.05 observed. At variance in the H^- model, the H^- products mainly originate from the final part of the trajectory leading to a prediction of 0.4 emitted electrons [full line in Fig. 1(b)], in reasonable agreement with the experiment. This concludes in favor of electron emission mainly through cycles of attachment and detachment processes, without excluding a weak contribution from the promotion model. Of course, if the promotion model is modified to produce a large fraction of negative ions which could detach their electrons, then both models could fit our data.

Since excitons are not associated with electron emission, the above evidence of an H^- precursor does not necessarily apply to the exciton population mechanism. Yet H^- ions probably couple efficiently with the exciton states. Because of the Coulombic attraction between the receding H^- ion and the F^0 atom appearing as a positive charge within the Madelung potential, the H^- level crosses that of the exciton(s) (Fig. 3). Since the H^- and the exciton wave functions probably have comparable spatial extension, one expects a large resonant electron transfer rate at the curve crossing. In this local description, the branching ratio **B** is interpreted as the transfer efficiency at the curve crossing. At each F^- site where an electron has been captured on H^-, a fraction $\mathbf{B} = 40\%$ of the H^- ions manage to escape from the capture site, whereas $1 - \mathbf{B} = 60\%$ lose their electron to the exciton states.

Finally, the present study suggests that the probability for an H^- ion to detach its electron is very large and on the order of 40% to 50% per lattice site. We propose that

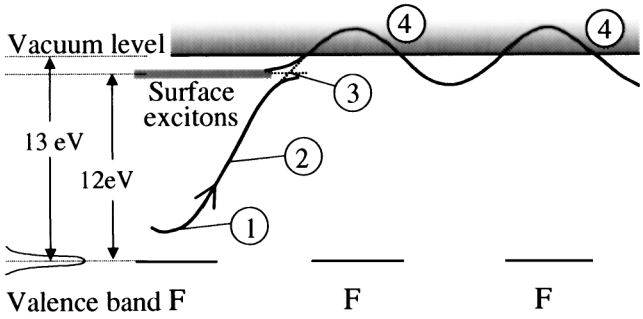

FIG. 3. Schematic representation of potential energies experienced by the H^- ion along its trajectory close to the surface. First, at close distance to an F^- center, electron capture takes place onto H^- (1). The Coulomb attraction raises the $H^- + F^0$ level (2). When leaving the lattice site electron transfer to the exciton level can occur (3). The H^- that passes the crossing is efficiently detached at the next F^- site (4). The energies measured in this experiment are indicated on the left side.

the broad structure in the electron spectrum arises from a direct detachment process of the H^- ion nearby the subsequent F^- sites (Fig. 3), where the overlap between the wave functions "pushes" away the loosely bound electron. Since F^- in the lattice should be regarded as a closed shell species, this process is basically similar to the isoelectronic H^--Ne atomic system for which a large cross section has been measured in the gas phase [22].

Large attachment probabilities have been calculated for oxygen and fluorine projectiles [13,14]. However, only the threshold behavior with projectile velocity could be compared with experiments since the final charge state derives from a dynamical equilibrium where destruction of the negative ion is very likely. As for the detachment process, it is usually not considered in the interpretation of experimental or theoretical results of negative ion fractions at low energies. Only at higher velocity, where the experimental yields fall off, the electron loss has been interpreted as being due to a coupling with the Li^+ conduction band [23].

In conclusion, a new coincidence technique has been applied to investigate the correlation between projectile charge state and electron emission in proton-LiF(100) interaction. The significant energy loss and electron emission observed are dominated if not fully driven by the formation of negative ions. The large value of the band gap is bypassed by the moderate energy defect associated with the electron capture to the H^- level shifted down by the Madelung potential [13]. The dominant energy loss mechanism is not associated with electron emission but corresponds to leaving the extracted electrons bound to the surface by 1 eV. We interpret this as the population of surface excitons, probably via recapture of the H^- electron at the same halogen site where it has just been captured. Electron emission is the consequence of the direct detachment into vacuum of the negative ions. In this dynamical context where only a minor fraction of the H^- ions leave the surface, the energy loss spectra are well reproduced by a simple model based on trajectories spanning over ten lattice sites and a reduced set of average probabilities. At each site an electron attachment probability of 15% is derived, among which 60% end up in surface excitons. The remaining H^- ions, which survived the capture site, further detach their electron with 40%–50% probability per site. Each of these probabilities may be directly compared with calculations.

Finally, the results address the recurrent question of the effective electronic structure at the surface. We find 13 ± 0.3 eV for the center of the LiF valence band with respect to vacuum level and a surface exciton band centered at 11.9 ± 0.2 eV above the center of the valence band. New measurements with an improved energy resolution should allow a more sensitive evaluation of the effective location and widths of the levels involved.

The authors are indebted to M. Barat for continuous interest and for suggestions while writing the manuscript. Fruitful discussions with A. Borisov, J. P. Gauyacq, and V. Sidis have played an important role in this work. H. Winter, C. Auth, and A. Mertens are kindly acknowledged for communicating their results prior to publication.

*Corresponding author.
Electronic address: roncin@lcam.u-psud.fr

[1] R. Souda *et al.*, Phys. Rev. Lett. **61**, 2705 (1988).
[2] M. Vana *et al.*, Europhys. Lett. **29**, 55 (1995).
[3] J. Limburg *et al.*, Phys. Rev. Lett. **75**, 217 (1995).
[4] C. Auth *et al.*, Phys. Rev. Lett. **74**, 5244 (1995).
[5] R. Souda *et al.*, Phys. Rev. B **50**, 18 489 (1994).
[6] C. Auth, A. G. Borisov, and H. Winter, Phys. Rev. Lett. **75**, 2292 (1995).
[7] L. Hägg, C. O. Reinhold, and J. Burgdörfer, Phys. Rev. A **55**, 2097 (1997).
[8] C. Auth *et al.*, Phys. Rev. Lett. **81**, 4831 (1998).
[9] K. Eder *et al.*, Phys. Rev. Lett. **79**, 4112 (1997).
[10] A. Mertens *et al.*, Phys. Rev. A **55**, R846 (1997).
[11] A. G. Borisov, V. Sidis, and H. Winter, Phys. Rev. Lett. **77**, 1893 (1996).
[12] F. W. Meyer *et al.*, Nucl. Instrum. Methods Phys. Res., Sect. B **125**, 138 (1997).
[13] A. G. Borisov and V. Sidis, Phys. Rev. B **56**, 10 628 (1997).
[14] C. Auth *et al.*, Phys. Rev. A **57**, 351 (1998).
[15] P. Stracke *et al.*, Nucl. Instrum. Methods Phys. Res., Sect. B **125**, 67 (1997).
[16] V. A. Morosov *et al.*, Rev. Sci. Instrum. **67**, 2163 (1996).
[17] J. Villette *et al.* (to be published).
[18] A. G. Borisov *et al.* (to be published).
[19] D. Ochs *et al.*, Surf. Sci. **383**, 162 (1997).
[20] P. Wurz *et al.*, Phys. Rev. B **43**, 6729 (1991).
[21] P. A. Cox and A. A. Williams, Surf. Sci. **175**, L782 (1986).
[22] W. Esaulov, D. Dhuick, and J. P. Gauyacq, J. Phys. B **11**, 1049 (1978).
[23] N. Lorente *et al.*, Nucl. Instrum. Methods Phys. Res., Sect. B **125**, 277 (1997).